AIAA SciTech Forum
January 3-7, 2022, San Diego, CA & Virtual
AIAA SCITECH 2022 Forum
10.2514/6.2022-0316

On the Feasibility of Using the Interplanetary Solar Wind Plasma Flow to Generate Electricity for Spacecraft

Chris N. Torre[1] and William V. Torre[2]
Torre Space Power Systems, Sherwood, AR 72120, USA

Daoru Han[3]
Missouri University of Science and Technology, Rolla, Missouri, 65409, USA

This paper explores the feasibility of a different method of power generation for spacecraft with a higher power density per weight and volume than conventional forms of spacecraft electrical power generation. The flow of interplanetary space plasma ions, when guided through a perpendicular magnetic field, can generate voltage that is picked up by electrode plates using a process known as Magnetohydrodynamics (MHD) generation. This results in an electrical current that could be used to power space-based orbiting satellites, probes, stations, habitations, and interplanetary missions to charge batteries, power communications, propulsion, guidance, navigation and control.

I. Nomenclature

A	=	cross-sectional area		
AU	=	Astronomical Unit	=	1.496 E+13 cm
Å	=	Angstrom Unit	=	10E-10 m
c	=	speed of light	=	2.9979 E+10 cm/sec
B	=	magnetic field strength	=	J/amp-m^2 (Tesla)
C	=	coulombs		
C_p	=	specific heat at constant pressure		
C_v	=	specific heat at constant volume		
dt	=	time step		
e	=	electron unit of charge	=	1.602E-19 coulomb
h	=	height		
J	=	Joule	=	1 N-m = kg-m2/s2
k	=	ratio of specific heats		
°K	=	degrees Kelvin		
K_B	=	Boltzmann Constant	=	1.38064852 E-23 J/°K
kg	=	kilogram		
Kn	=	Knudsen number		
L	=	length or size dimension		
m	=	meter		
ṁ	=	mass flow rate, kg/sec		
$m_{electron}$	=	mass of electron	=	9.109 E-31 kg
m_{proton}	=	mass of proton	=	1.673 E-27 kg
MHD	=	Magnetohydrodynamic		
mho	=	electrical conductivity	=	ohm^{-1} (1.0 Siemens)
n	=	ion density		

[1] Senior Aerospace Engineer, Spacecraft Systems, AIAA Member.
[2] Principal Investigator, Senior Electrical Engineer, IEEE Member.
[3] Assistant Professor of Aerospace Engineering, AIAA Senior Member.

Copyright © 2022 by the American Institute of Aeronautics and Astronautics, Inc. All rights reserved.

Downloaded by Chris Torre on December 30, 2021 | http://arc.aiaa.org | DOI: 10.2514/6.2022-0316

N_A	=	Avagadro's number	=	6.0221 E+23/mole
n_e	=	electron density		
P	=	pressure, pascal		
Pr	=	Prandtl number		
PV	=	photovoltaic		
R	=	Universal Gas Constant	=	8314.472 Joules/kgmole-°K
Re	=	Reynolds number		
Rm	=	Magnetic Reynolds number		
R_Θ	=	solar radius	=	6.9599 E+10 cm
S/A	=	Solar Array		
T_e	=	electron temperature		
V	=	velocity (m/sec or km/sec)		
W	=	watt		
x	=	distance		
δ	=	Rarefaction parameter		
ϵ	=	density parameter		
ε_0	=	permittivity of free space	=	8.854 E-12 C^2/Nm^2
λ	=	mean free path		
λ_D	=	Debye Length		
ρ	=	density (particles/m^3)		
σ_0	=	electrical conductivity (mho)		
μ	=	dynamic viscosity		
ν	=	kinematic viscosity		
ν_m	=	molecular velocity		

II. Introduction

The feasibility of extracting energy from space plasma (solar wind) depends on a combination of functions working together: sufficient kinetic energy and electrical continuity being provided within the interplanetary plasma, an electrical system to convert plasma energy into a usable current, a power regulation system to match power generated with spacecraft power demand, and a control of the voltage range generated with a battery storage system. These essential elements must be compact and economically viable when compared to other power systems and understandable in principle. Based on the analysis summarized herein, the capability of an MHD generation system is expected to produce significantly more power with less weight (W/kg) and volume (W/m^3) densities than solar photovoltaic (PV) panels, thereby reducing launch payload and cost. An MHD generation system could also provide continuous power generation even when blocked by sunlight, unlike PV, thereby reducing reliance on energy storage. An MHD generator has the benefit of no moving parts to produce electrical energy and essentially consists of a channel through which ionized particles are passed through an applied magnetic field. Electrodes collect a voltage potential perpendicular to the magnetic field and the flow of ionized particles as depicted here in Fig. 1. The power output of this MHD generator is proportional to the product of the plasma conductivity, the square of the ionized plasma velocity, and the square of the strength of the magnetic field through which the plasma passes, as will be seen below. For space-based applications a convergent inlet nozzle could increase the density and conductivity of ionized plasma while accelerating the velocity of electrons and protons.

This paper describes the analyses that have been performed based on plasma conditions recorded by various space probes and a summary of a planned test article for both LEO and Solar Wind plasma environments. The following system description is divided into three parts: the solar wind plasma characteristics, the electrical system design, and the mechanical components description.

A. Space Plasma Characteristics

The solar wind is a mixture of ionized plasma which originates from the sun and composed of mainly electrons and protons with approximately an 8% component of helium (alpha particles) and trace amounts of heavy ions and atomic nuclei: C, N, O, Ne, Mg, Si, S, and Fe [1] ripped apart by heating of the Sun's outer atmosphere, the corona. This evaluation herein assumes that MHD generator performance is dependent on the electrons and protons of the solar wind (not heavy ions) as these make up about 92% of the solar wind (Feldman, et al.) [2]. The flow of ions is considered frictionless (inviscid) with minimal boundary layer effects and the equation of state can be represented by the ideal gas law: $pV = nRT$. The flow of ions is isentropic (at constant entropy). As a result, the flow can be

Downloaded by Chris Torre on December 30, 2021 | http://arc.aiaa.org | DOI: 10.2514/6.2022-0316

Downloaded by Chris Torre on December 30, 2021 | http://arc.aiaa.org | DOI: 10.2514/6.2022-0316

considered frictionless with no dissipative losses and adiabatic since no heat or mass enters of leaves the system [3]. The flow is highly compressible since the pressure and density are rarefied in the space plasma and the Mach number is very high. The flow is considered to be Quasi-One dimensional as the properties aren't varied across the width of the MHD channel. Only variation along the x-axis is considered here for simplification because the highly energetic ions are likely bounce off the walls of the interior components and are affected by magnetic fields. The plasma is flowing radially away from the sun with measured property and velocity ranges shown in Fig. 2.

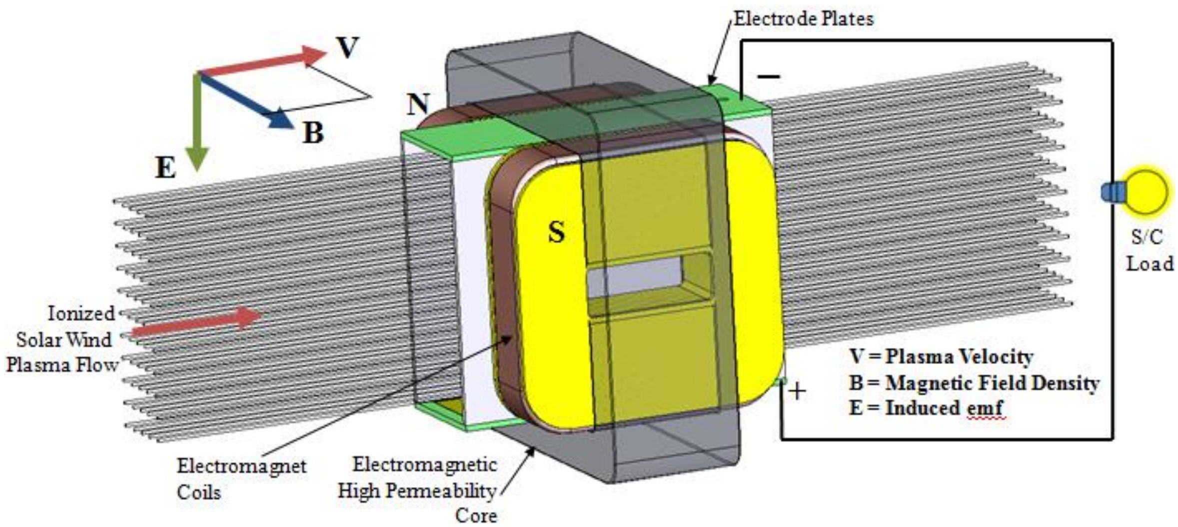

Figure 1. MHD Generator Principle

III. Generator System Description

Transients in the Solar Wind consist of variations in the proton and electron pressure balance, as described by Burlaga and Solodyna, et. al., [4] and are due to directional discontinuities that cause speed changes with zero or small changes in density and magnetic field directions (using Pioneer 10 & 11 data, then approx. 41/day @ 1 AU, 0.5/day @ 30 AU). And due to tangential discontinuities of a scale size ~ .01 AU (~ 1 hr) (from Pioneer 6) in which the pressure is constant, the change in density is zero and creates velocity shear component with no normal component, and some magnetic field direction changes. There are rotational discontinuities in which the change in density is zero and the magnetic field direction changes, plus various microscale waves and turbulence perturbations in the solar wind, e.g. magnetic field holes, small directional changes and stream interface changes.

P_0	≈ 1.3 E-11 Pa ≈ 1.89 E-15 psi	[5 & 6]
Tev	≈ 1.4E+05 °K from Helios data	[7]
ρ_0 ρ_{0rms}	≈ 4.2 E+06 ion/m3 ≈ 7.14E-21 kgm/m3 ≈ about 4 to 8 electrons/cm3 ≈ 6 /cm3	[8]
m_{proton} $m_{electron}$	≈ 1.673 E-27 kg ≈ 9.109 E-31 kg	[9]

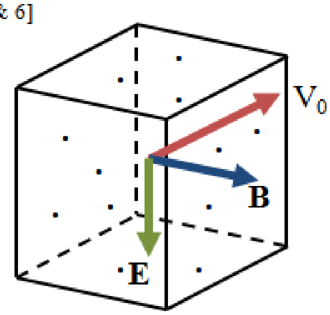

V_0max V_0avg V_0min	= 0.8 E+06 m/sec = 0.6 E+06 m/sec = 0.4 E+06 m/sec	[10]
V_0	= 412 – 409 km/s from Vela 3, IMP-3, IMP-7, and IMP-8 data	[11]
V_0	= 468 km/s = 468,000 m/s	[12]

Figure 2. Plasma Properties.

A.1 Flow Regime Characterization

Since the solar plasma has an ultra-low density and pressure, then determination of the flow through the MHD channel uses the kinetic approach with principles drawn from rarefied gas dynamics due to the small density of ion particles. This flow behavior will be different from a general gas wherein the number of molecules is large enough to consider the gas as a continuum medium that is not valid here if the flow behaves as a free molecular flow largely without collisions. The flow regime is thus characterized according to its Knudsen number, Kn, which is the ratio of the molecular mean free path to a characteristic length of the system. With a Knudsen number > 0.5 there are almost no interactions between particles, and thus the ions would collide mainly with the walls of the MHD channel components. When Kn >> 1 then statistical mechanics apply. Fig. 3 represents a spectrum of flow regimes categorized by Knudsen number [Cf. also12]. The mean free path, λ, in rarefied gases is the "*average length of the rectilinear paths between molecular collisions*" [13].

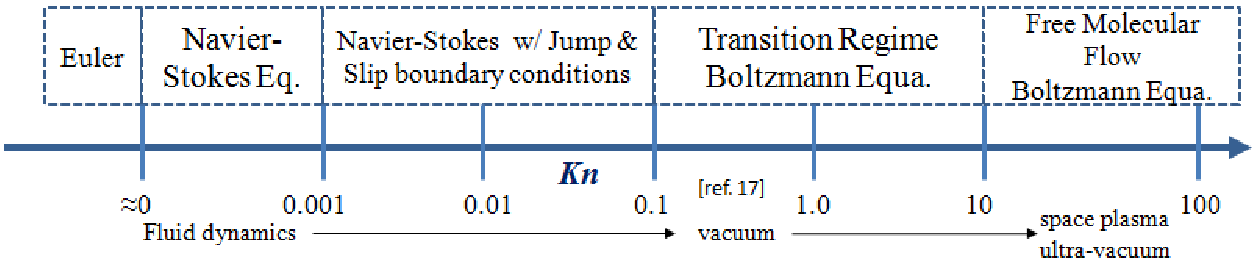

Figure 3. Flow Regimes by Knudsen Number.

The Knudsen number is defined in Eq. 1 as:

$$Kn = \frac{\lambda}{L} = \frac{mean\ free\ path}{characteristic\ length} \quad (1)$$

where the mean free path λ_e of electrons as a function of solar radius (R/R_Θ) has been evaluated from Helios and IMP data by Estel and Mann [14]. For R_Θ = 6.9599 E+10 cm and R = 1 AU = 1.496 E+13 cm [15], then $R/R_\Theta \approx$ 214 cm as the mean free path λ_e in the high vacuum of space, which is considered collsionless. The opening size, L, of a representative MHD channel may vary according to the system selection, but let's say it is 5.0 cm. Then the electron Knudsen number is: $Kn_e = \lambda_e /L = (R/R_\Theta)/L$ = 214/5.0 = 42.8. And the Rarefaction parameter is δ = 1/Kn = 0.024 which corresponds to a free molecular region [16]. Large values of δ correspond to the hydrodynamic regime and small values of δ are appropriate to the free-molecular regime. This parameter is sometimes more convenient because many solutions are given in terms of this parameter. Similarly, the mean free path of protons can be found as a function of AU distance from Ulysses data evaluated by Erdos, Balogh and Kota [17]. Thus the Knudsen number of protons can be approximated as: $Kn_p = \lambda_p/L$ = 0.04(1.496 E+13 cm)/5.08 cm = 3.0E+9.

The Prandlt number, on the basis of kinetic theory, of the free stream approaching the MHD channel passage, is defined here in Eq. 2 [18]:

$$Pr = \frac{momentum\ diffusivity}{thermal\ diffusivity} = \frac{\nu}{\alpha} = \frac{\mu/\rho}{k/(c_p\rho)} = \frac{c_p\mu}{k} = \frac{4k}{9k-5} = 0.666 \text{ to } 1.0 \quad (2)$$

wherein the gas constant k (ratio of specific heats) = cp/cv and for simple gases $k = (n+2)/n$ and monatomic gases O and N have n = 3 and k = 1.66 [19]. Carroll and Ostlie indicate that k = 5/3 (1.667) for ideal monatomic gases [20]. Another source finds cp = 20.8 J/mol-K *and* cv = 12.5 J/mol-K, thus k = 1.664 [21].

The Reynolds number within the length of an MHD channel passage can be found from Eq. 3 [22]:

$$Re = \frac{\rho VL}{\mu} = \frac{VL}{\nu} \quad (3)$$

It should be noted that viscosities μ and ν are everywhere unknown in the space plasma, and ρ varies considerably, so "*transport properties, such as viscosity and thermal conduction, of the intergalactic plasma … are largely unknown"* [23]. Noting this lack of viscosity data, a reasonable assumption may be that the kinematic viscosity ν is an extremely small value which leads to high Reynolds numbers in the range of somewhere around 1.00 E+28 which is >> 1, using the velocity range shown in Fig. 2 and a representative passage length of 5.0 cm. The magnetic Reynolds number (Rm) is the magnetic analogue of Re which provides an estimate of the relative effects of advection or induction of a magnetic field by the motion of a conducting medium to magnetic diffusion [24]. The magnetic Reynolds number is important in determining how plasma is to the magnetic field lines and for scaling purposes. This quantity is given by $Rm = \mu_0 LV\sigma$, where L is the characteristic length, V is the characterization velocity, and σ is the electric conductivity of the plasma, and , in this case, μ_0 is the magnetic permeability of free space.

The Density Parameter is given by Eq. 4 [25]:

$$\epsilon = d^3 n \quad (4)$$

where: $d \approx 1$Å

Downloaded by Chris Torre on December 30, 2021 | http://arc.aiaa.org | DOI: 10.2514/6.2022-0316

so: ϵ = (10E-10m)^3(4.2 E+06 ion/m^3) = 4.2 E-21 << 1,
whereas in the earth's standard atmosphere: ϵ = 1.4 E-3

The Debye Length λ_D depends on the electron energy and the density of the plasma and is found by Eq. 5 [26 & 27]:

$$\lambda_D = \left(\frac{\epsilon_0 K T_e}{n e^2}\right)^{\frac{1}{2}} \quad (5)$$

where: ε_0 is the permittivity of free space
K_B is the Boltzmann constant
e is the elementary electron charge
T_e is the electron temperature
n is the density of electrons

The temperatures for electrons and heavier ions may differ and the background medium can be treated as the vacuum. The Debye length in the solar wind and interstellar medium is ~10 m [28]. Since a spacecraft size could be ~ 10's of meters, then the ratio of the length of a representative size of a spacecraft length L to the Debye length is approximately L > λ_D depending on design specifics of a spacecraft, which is indicative of a collisionless plasma.

A.2 Approximation of the Flow Rate Through the Channel

If we consider the free stream entering the MHD channel from the basic perspective of the continuity equation and conservation of momentum, then, with an opening as shown simplified here in Fig. 4, the mass flow rate $\dot{m}_1$ is of the plasma flowing directly into the channel without benefit of a convergent inlet nozzle. Whereas the mass flow rate $\dot{m}_0$ is the rate of the plasma flowing into a larger diameter of a convergent inlet nozzle if the MHD Channel is preceded by such a nozzle, thus $\dot{m}_1$ would be larger. The mass flow rate $\dot{m}_2$ is equivalent to $\dot{m}_1$ since there are no losses and momentum is conserved. So with no added benefit of a front inlet scoop to increase $\dot{m}_1$, then $\dot{m}_1$ is here in Eq. 6:

$$\dot{m}_1 = \rho_0 \bullet V_0\text{avg} \bullet A_1 \bullet m_{\text{electron}} \quad (6)$$

For example, the mass flow rate of the fraction of electrons in the plasma would be somewhere around $\dot{m}_1$ = 4.2 E+06 /m^3 • 0.5 E+06 m/sec • 0.0020 m^2 • 9.109 E-31 kg = 3.26 E-21 kg/sec for a 0.2 cm^2 opening And the mass flow rate of protons would be approximately $\dot{m}_1$ = 1.0 E+06 /m^3 • 0.5 E+06 m/sec • 0.0020 m^2 • 1.673 E-23 kg = 1.673 E-14 kg/sec for a 0.2 cm^2 opening. Of course in practice the mass flow rate would be calculated according to the specifics of system application requirements.

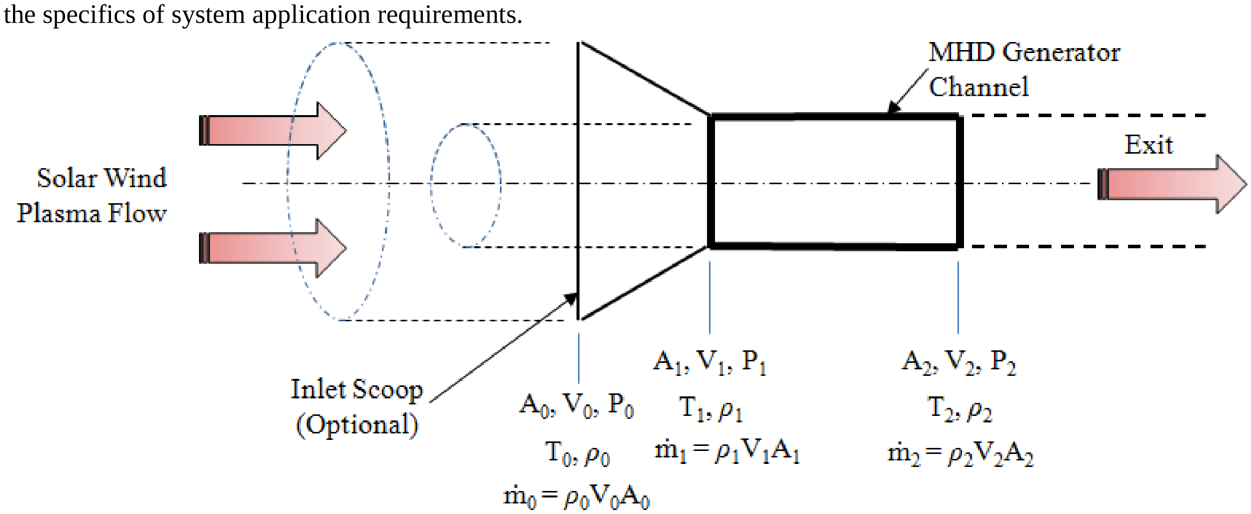

Figure 4. MHD Channel Flow Diagram.

However, since the plasma is an extremely rarefied, collisionless gas, then one method to estimate the maximum flow rate capability of rarefied gas through the MHD channel can be estimated by the so-called velocity slip and temperature jump boundary conditions. This means that the bulk velocity is not equal to zero on the wall, but its tangential component near the wall is proportional to its normal gradient. This has been evaluated by Sharipov [29] (and others) for vacuum systems and summarized here in Eq. 7:

$$\dot{m} = \frac{\pi a^2 P}{v_m}(G_T \xi_T - G_P \xi_P) \quad (7)$$

Downloaded by Chris Torre on December 30, 2021 | http://arc.aiaa.org | DOI: 10.2514/6.2022-0316

Downloaded by Chris Torre on December 30, 2021 | http://arc.aiaa.org | DOI: 10.2514/6.2022-0316

From this, the maximum mass flow rate capability of the MHD channel can be calculated with appropriate selection of gradient factors, flow coefficients and the selection of MHD channel geometry. Small longitudinal gradient factors for pressure and temperature are defined by Eq.'s 8 and 9 [30]:

$$\xi_P = \frac{a}{P}\frac{dP}{dx} = \frac{a}{P}\frac{\Delta P}{\Delta x} \quad (8)$$

$$\xi_T = \frac{a}{T}\frac{dT}{dx} = \frac{a}{T}\frac{\Delta T}{\Delta x} \quad (9)$$

and flow coefficients are defined in Eq.'s 10 and 11 [31]:

$$G_P = \frac{\delta}{4} + \sigma_P \quad (10)$$

$$G_T = \frac{\sigma_T}{\delta} \quad (11)$$

where: δ = Rarefaction Parameter,
σ_P = velocity slip coefficient
σ_T = temperature jump coefficient

and the most probable molecular velocity ≈ 1.88 E+06 m/sec from Eq. 12 [32]:

$$v_m = \sqrt{\frac{2RT}{m}} \quad (12)$$

where: R= 8314 J/kg-°K universal gas constant
$T \approx$ 2.7 to 116 °K,, an approximation of the ambient temp. of plasma [33 & 34] and
m = molecular mass of electrons = 6.022 E+23 electrons/mole X 9.109 E-31 kg/electron = 5.485 E-07 kg.

The results of this method are plotted in Fig. 5 with the values of calculated $\dot{m}_1$ vs. an MHD inlet channel opening Area A_1. The higher flow rate capability from Eq. 7 of rarefied plasma through a channel exceeds the nominally calculated amount of mass flow rate based on Eq. 6 above. For comparison, the mass flow rate of a rarefied helium medium at the same pressure and temperature is shown for reference.

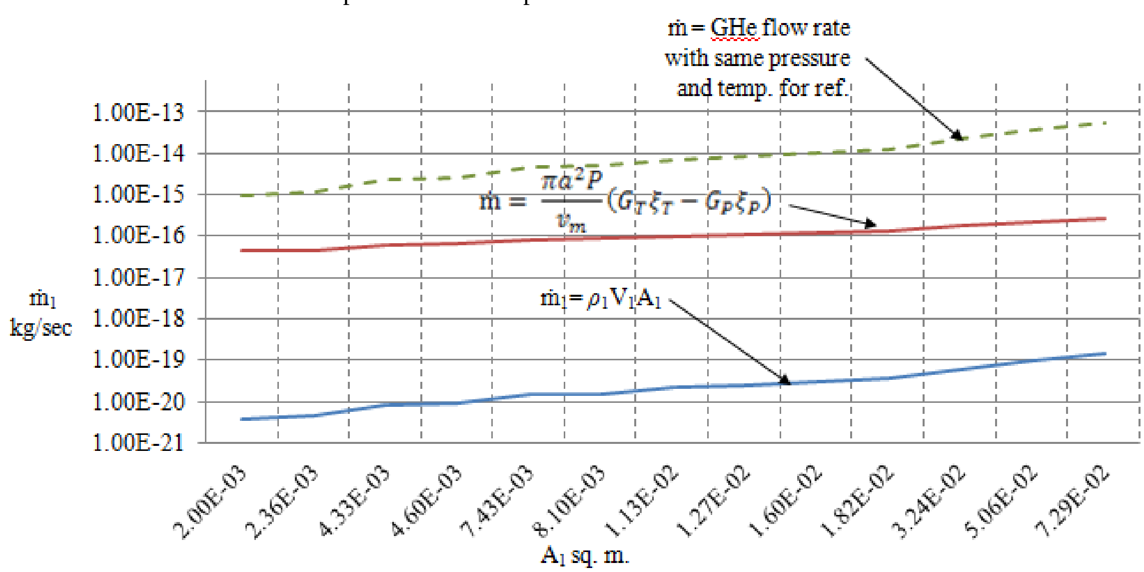

Figure 5. Mass Flow Rate Approximations.

However, from the Knudsen number and Debye Length values calculated, a collisionless plasma needs a kinetic approach to achieve a real sense of particle modeling behavior. Particle-In-Cell (PIC) is a technique used to simulate motion of plasma particle flows with high Knudsen numbers that cannot be treated with classic continuum methods, as represented for example by the Navier–Stokes or the magnetohydrodynamic equations. Instead, the more fundamental Boltzmann equation has to be solved, which is done approximately by particle based methods. The PIC method is used to treat the collisionless Vlasov–Maxwell system, while neutral reactive flows are treated by the Direct Simulation Monte Carlo (DSMC) method. [35] The flow is collisionless; (e.g., $(\partial f/\partial t)_{coll} = 0$, and the only external force F considered is the Lorentz force) and the particles are finite-sized with no interactions between them.

A.3 Plasma Electrical Conductivity

The electrical conductivity of the plasma is determined by ion mass, plasma density, and charge of the ionized particles. In LEO the ionized particles are mainly free electrons and in the solar wind the plasma consists of a mix of electrons and protons. The electrical conductivity of the plasma in the free stream around 1AU has been traditionally determined from Eq. 13 [36]:

$$\sigma_0 = \frac{n_e e^2}{m_e \nu} \quad (13)$$

where: σ_0 = plasma conductivity
n_e = Electron density ≈ 4.2E+06 ion/m^3
e = Atomic unit of charge = 1.6E-19 coulombs
m_e = Electron mass = 9.1E-31 kg

Space plasmas have low collision rates, thus, for the purposes of this calculation, we can determine the collision frequency as [37]:

where: ν = collision frequency (1/s) = 5.64E-04 sec^{-1}
ν = collision frequency (1/s) = (2.91 E-06) X lnΔ X Te = 4.365 E-05 sec^{-1}
lnΔ =15 = Coulomb Logarithm (7 – 15 range typ)
Te= 1eV = electron kinetic temperature

Based on data collected from the Van Allen probes, the electron temperature is generally .2 – 2 eV (2000 – 20,000 K).

$$\sigma_0 = 209.35 \text{ mhos/m}$$

It has also been calculated by Wilson, et. al., that collision rates can vary within: 7E-08 sec^{-1} < ν < 4E-06 sec^{-1} and that the electron kinetic temperatures can vary from: Te ≈ 0.23 to 12.4 eV for all time periods [38], which would indicate a wide variance in conductivity values.

B. Electrical System Design

B.1 System Description

Fig. 6 depicts the major interconnected elements of an MHD electrical system starting with the entry of particle flux plasma flowing through a channel which has one electrode mounted on the top and another electrode mounted 180 degrees apart on the bottom, and electromagnets mounted on the sides that are spaced 90 degrees rotationally from the electrodes.

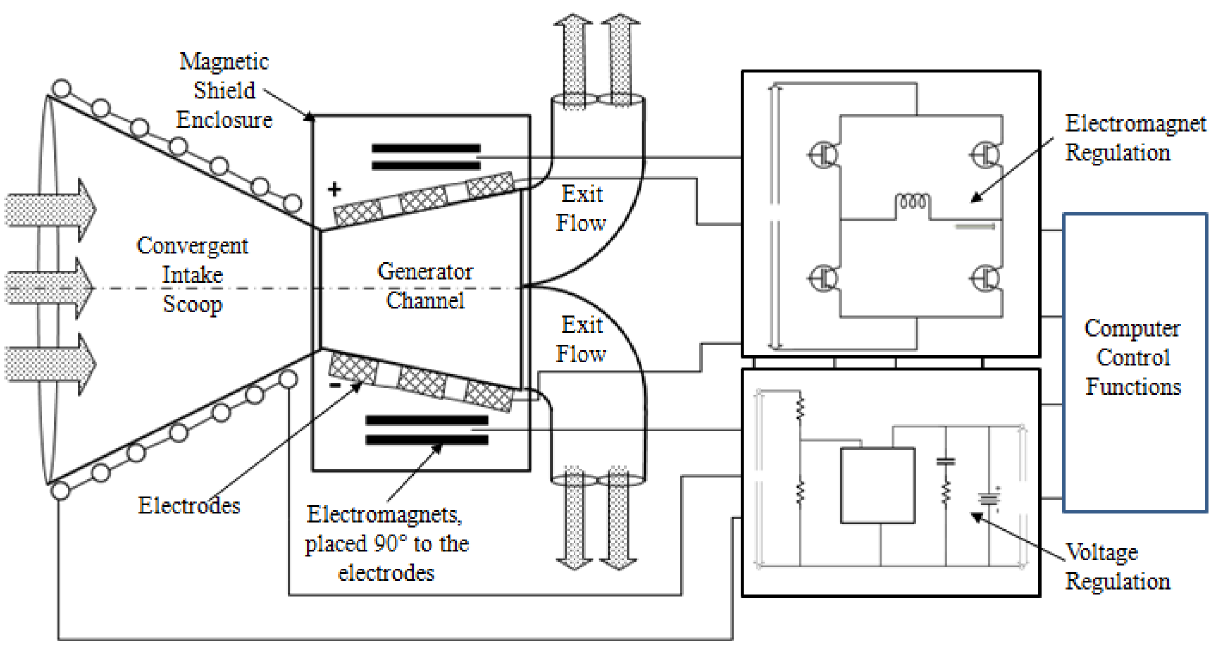

Figure 6. Electrical System Elements.

Downloaded by Chris Torre on December 30, 2021 | http://arc.aiaa.org | DOI: 10.2514/6.2022-0316

The electrically charged plasma creates a charge flow across the electrodes from positive toward negative. The DC voltage that is created flows to a linear voltage regulator circuit within a power module to control the input voltage to the battery and other spacecraft functions (27 vdc is commonly used as the principal bus voltage on most spacecraft) via a connection between the MHD generator system and the spacecraft bus electrical system which is used for guidance, navigation and control, instrumentations, and communication. A computer, with software, controls and monitors MHD generation functions, including three control loops for voltage regulation, power regulation, ion scoop voltage, and receives data from a Faraday cup (mounted separately aboard the spacecraft) for plasma measurement.

B.2 Power Generation

The basic equation for power output from MHD generation is shown below in Eq. 14, which can be used to analyze the MHD generator performance for various configurations of MHD channel size, magnetic field strength, and plasma scoop size for applications from a small satellite system size to larger versions that can produce higher power. This is the basic equation for estimating performance based on MHD channel geometry, electromagnet field strength, and plasma conditions. In addition to the main electromagnet(s), a small permanent magnet could be positioned to project a magnetic field orthogonal to the flow of the direction of the ionized plasma to assist in generating an initial magnetic field during startup.

$$P = \frac{U^2 B^2 \sigma}{4}(A\delta) \qquad (14) \quad [39]$$

where: P = Total Power Output (Watts)
U = Velocity of Plasma ions (m/s)
B = Magnetic field strength (Tesla)
$\boldsymbol{\sigma}$ = Conductivity of plasma (mho/m, the inverse of resistance)
A = Electrode surface (m^2)
$\boldsymbol{\delta}$ = Distance between electrodes (m)

The efficiency of a Faraday MHD generator is determined by Eq. 15 shown below. The two primary variables affecting the MHD generator efficiency is the electrode separation distance (δ) and the plasma conductivity ($\boldsymbol{\sigma}$). Greater electrode separation results in higher efficiency from increased plasma volume. The conductivity of the plasma is determined by the available ionized plasma density and energy in space and the size of the ion scoop.

$$n_c = \delta(1 - \frac{\delta}{2\sigma}) \qquad (15) \quad [40]$$

where: n_c = efficiency, %
$\boldsymbol{\delta}$ = Distance between electrodes (m)
$\boldsymbol{\sigma}$ = conductivity of plasma (mho/m)

B.3 Magnetic Field Strength

The MHD generator power output is proportional to the square of plasma velocity, and the magnetic field strength produced by the electromagnet, and directly proportional to the plasma conductivity and distance the electrodes are separated. The magnetic field produced by the electromagnet is a variable that can be controlled and adjusted to change the amount of power that is being generated. The magnetic field strength is directly proportional to the amount of current that is circulated through the electromagnet, as shown in equation 16. An electromagnet needs to be chosen with a solenoid coil which will have a high magnetic permeability.

$$B = \mu N I \qquad (16) \quad [41]$$

where: B = Magnetic field strength (Tesla)
μ = magnetic permeability (T amp/m)
N = number of turns of coil
I = Amps

The power regulation control is designed to control the current flow through the magnet and thus control the magnetic field and power produced by the MHD generator.

B.4 Open Circuit Voltage

The DC voltage produced at the MHD channel electrodes would be directly proportional to the ion particle velocity in the MHD channel, the distance between the anode and cathode, and the magnetic field strength created

Downloaded by Chris Torre on December 30, 2021 | http://arc.aiaa.org | DOI: 10.2514/6.2022-0316

by the electromagnet. This voltage produced at the electrodes can vary if any of these variables change significantly. The equation for the calculation of open circuit voltage is shown in equation 17 below.

$$Voc = B \times \nu \times \delta \quad (17) \quad [42]$$

where: Voc = open circuit voltage
B = Magnetic field strength of electromagnet (Tesla)
ν = ion particle velocity (meters/ second)
δ = electrode separation distance (meters)

A constant voltage is needed for the spacecraft onboard power to maintain operations. The onboard electronics operate within a fairly tight voltage regulation (< 2-3 %). In LEO the ion particle velocity is primarily determined by the orbital speed of the spacecraft and is not expected to vary significantly after insertion into orbit. In GEO and deep space the solar wind ion particle velocity can vary significantly. The distance between electrode plates is constant, and the magnetic field strength from the electromagnet will be changing due to the power regulation control circuit, which will be automatically adjusting power output to match changing spacecraft load and variations in the plasma characteristics. Because of these variations in the magnetic field strength and plasma conditions, voltages at the electrodes will vary significantly. This hardware controlled voltage regulation control system with software control would adjust the voltage to the proper level and maintains a constant supply.

Downloaded by Chris Torre on December 30, 2021 | http://arc.aiaa.org | DOI: 10.2514/6.2022-0316

C. Mechanical Components Description

Figure 7 depicts some of the primary system elements of an MHD generator [Cf. also 43] with an inlet scoop. The chief functionality of any MHD channel geometry is that there be a component of the plasma velocity which is perpendicular to the magnetic field, so that a Faraday electric field V X B is created, where V = plasma velocity and B = magnetic field strength. Any moving conductor in a magnetic field will create a voltage potential orthogonal to the current flow on the conductor; thus when a closed loop is present current will flow. Collection and concentration of the space ionized plasma can be done by the use of an electromagnetic ion funnel [see ref.'s 44 and 45 for examples of ion funnels used in mass spectrometry] which collects and directs the ionized space plasma into a chamber that is configured as a simple Faraday channel with electrodes. The electromagnets are positioned to induce a magnetic field perpendicular to the flow of the ionized plasma. When the ionized conductive plasma flows through the channel, in the presence of the perpendicular magnetic field, ions will migrate due to the Lorentz forces from one anode electrode to the cathode electrode, thus generating a voltage potential with the electrodes placed 90 degrees to the magnetic field. The converging inlet scoop allows for precise positioning of the flow direction of ionized plasma, funneling, concentration and acceleration of the ion particles. This ion scoop has a series of spaced ring electrodes whose inner diameters gradually decrease, and serve to radially confine ions as they pass through. Out-of-phase RF potentials can be applied to adjacent rings and a DC voltage gradient applied along the axis of the ion scoop to drive ions into the MHD channel. This would result in higher ion plasma density and velocity, and increased conductivity with resulting plasma current flow to increase power output.

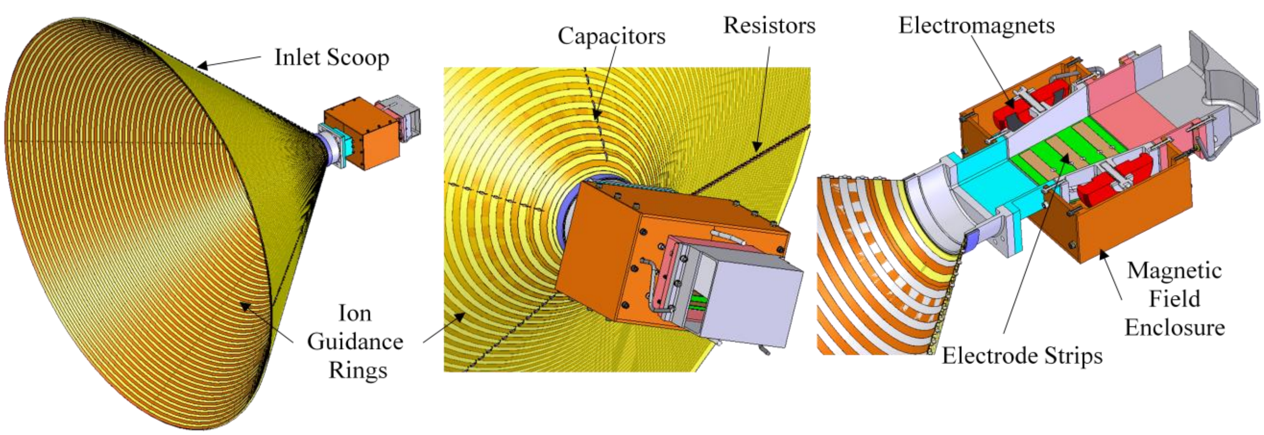

Figure 7. Primary Elements of an MHD Generator and Ion Inlet Scoop.

The electromagnet system is surrounded by a ferromagnetic alloy (commercially referred to as "Mu metal" [46]) metallic box with very high permeability to contain magnetic fields and shield them from influencing surrounding spacecraft RF fields in the vicinity of the MHD generator.

D. Cost and Weight Performance of an MHD Generator Compared to Solar Arrays

A characteristic of PV operation is that cells degrade over time due to exposure to atomic oxygen and free electron fluence. Thus there is a need for a spacecraft power source that has higher power density, increased reliability, and that can operate farther from the Sun. A comparison of MHD generation to PV solar generation is shown in Figure 8 for distances from the sun.

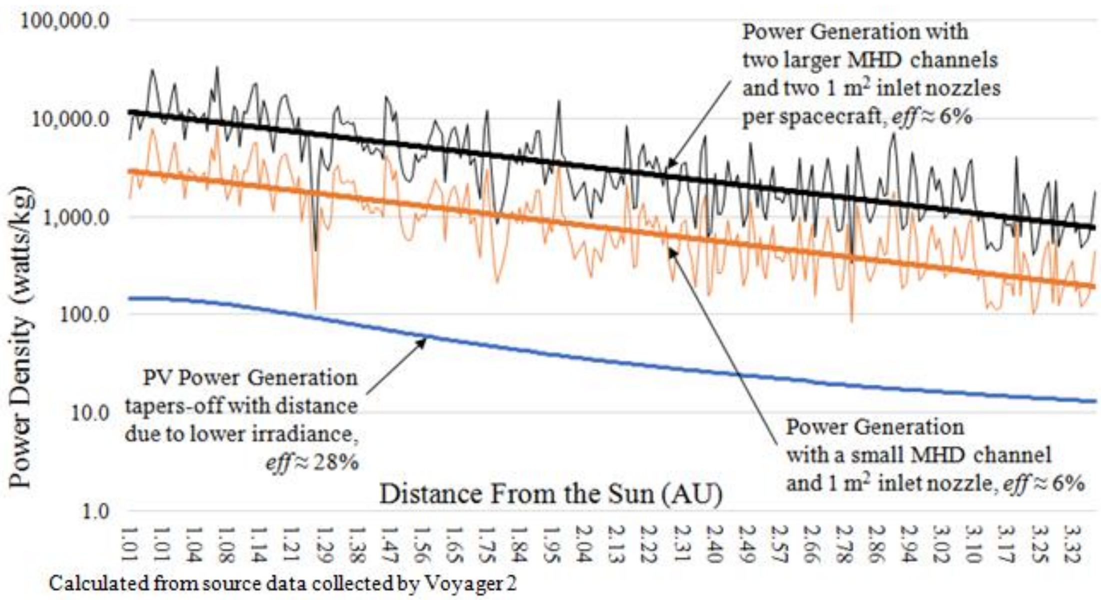

Figure 8. MHD vs. PV Power Density (W/kg).

The maximum values are based on the having all of the plasma parameters (ion density, particle collision frequency, temperature) at most favorable values to maximize MHD output power. Likewise, the minimum values are based on the possibility of occurrence of plasma conditions to be most unfavorable to MHD power production.

Figure 9 below depicts the historical trends of cost and mass for solar array systems together with

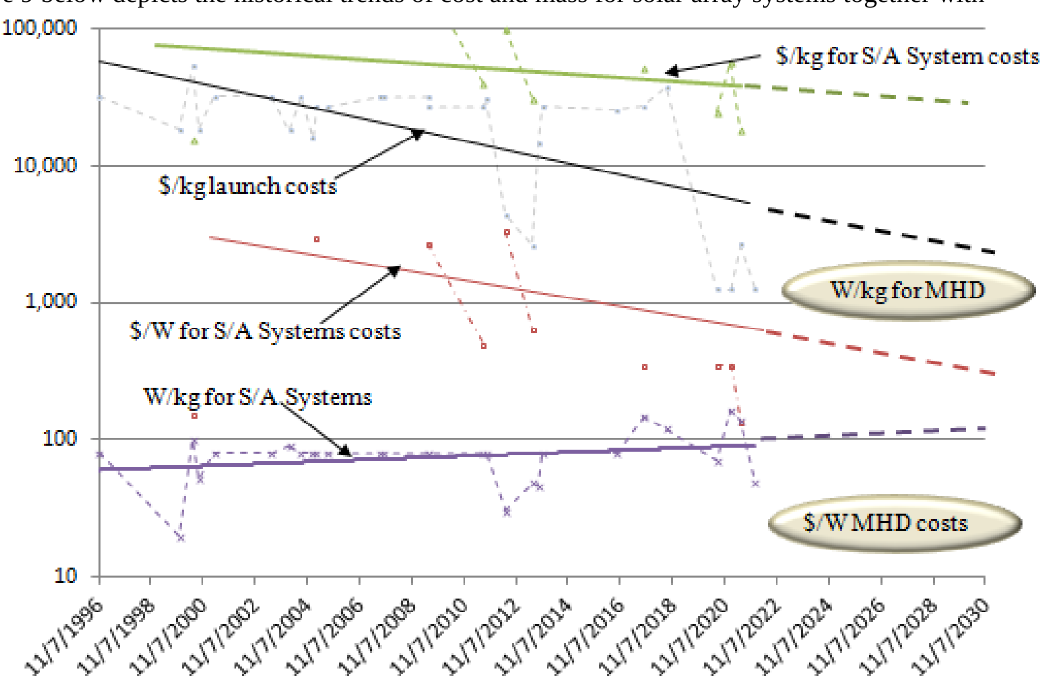

Figure 9. Relative Cost and Weight Trends for Solar Array PV Systems vs. MHD.

Downloaded by Chris Torre on December 30, 2021 | http://arc.aiaa.org | DOI: 10.2514/6.2022-0316

rocket launch costs [47-65]. It shows that there has been a downward trend in costs over time and a slight increase in power capability (W/kg) for S/A systems. The cost of $/kg launched varies widely due to negotiations, prices, supply & demand, customer requirements, and the number of payloads manifested per launch. These varying cost and requirements make market analysis imprecise. Also, solar panel array costs are difficult to find due to the manufacturer's proprietary restrictions, and differing form functional complexity and requirements. By comparison, MHD system costs are difficult to predict at this time but rough calculations show that the W/kg performance and $/W cost estimates of MHD systems should be in the zones of two bubbles.

IV. Conclusion

The technical viability and economic potential required to use MHD generation in space plasma on-orbit appears to be feasible based on the parameters evaluated above. With the development of computational fluid dynamics and other computer simulation tools the opportunities to explore an MHD generation system are open. More research investigation is required into various parts of an MHD system such as electrode design nuances, the effects of magnetic field forces and the general system geometry. The next logical step would be to construct a prototype and test it in a vacuum chamber with a simulated solar wind ion flow system that represents the densities and velocities of LEO and GEO environments with sufficient plasma diagnostics equipment. Scaling factors from the laboratory to the interplanetary plasmasphere need to be determined.

Commercial viability depends on the development of business models with risk mitigation plans that fit the interests of spacecraft power system needs and future mission concepts. Conventional solar array electrical generation capability tapers off due to lower irradiance at further distances from the sun, cells degrade over time due to exposure to atomic oxygen and free electron fluence, and dust mitigation needs for planetary body bases are important. Radioisotope power systems (RPS) can be attractive for outer planet missions and lunar or planet-based system concepts because RPS can be used in environments with limited or no sunlight; these are costly and not without environmental concerns. However, interplanetary and interstellar plasma is naturally abundant making the design of future mission systems that employ MHD power generation an opportunistic choice.

References

1. Wurz, Peter, "Solar Wind Composition," University of Bern, 2005, Proceedings of the 11th European Space Physics Meeting.
2. Feldman, W. C., in "Interplanetary Magnetohydrodynamics," by L. F. Burlaga, Oxford University Press, 1995, p. 36.
3. Benedict, R. P. and Steltz, W. G., "Thermodynamics of Compressible Fluids," 1963, p. 3.7.4-1.
4. Burlaga, Solodyna, et. al., "Interplanetary Magnetohydrodynamics," chapter 4, 1995, Oxford University Press.
5. "Introduction to Plasma Physics," P. Gibbon, Institute for Advanced Simulation, 2017, page 2.
6. Ibid., Burlaga, page 48, Voyager 2 data.
7. Ibid., Burlaga, page 35, Helios data.
8. Ogilvie, Gordon I., "Lecture Notes on Astrophysical Fluid Dynamics," 2016, University of Cambridge, page 10.
9. Pierrard, Vivienne, et. al., "Solar Wind Plasma Particles Organized by the Flow Speed," Solar Physics, Nov. 5, 2020.
10. Ibid., Burlaga, page 48 & 66 Voyager 2 data, page 59, and page 77 Explorer data.
11. Ness and Formisano in Burlaga, p. 37 and 48, from 1.0 AU to 2.1 AU.
12. Schwenn, 1990, recommended average in Burlaga, p. 43.
13. Sutton, George W., and Sherman, Arthur, "Engineering Magnetohydrodynamics," p. 5, 1965, McGraw-Hill Series in Mechanical Engineering.
14. Struchtrup, H. and Taheri, P., "Macroscopic Transport Models for Rarefied Gas Flows," Univ. or Victoria, Canada, 6 September 2010, in Journal of Applied Mathematics, 2011.
15. Estel, C. and Mann, G., "Mean Free Path and Energy Loss of Electrons in the Solar Corona and the Inner Heliosphere," 1999, Astronomy and Astrophysics.
16. Carroll and Ostlie, "Modern Astrophysics," 1996, Addison-Wesley, page A-1.
17. Scharipov, F., "Rarefied Gas Dynamics and its Applications to Vacuum Technology," Universidade Federal do Parana, Brazil, page 2.
18. Erdos, G., Balogh, A., and Kota, J., "Scattering Mean Free Path of Energetic Protons in the Heliosphere", 1996, Univ. of Utah, NASA Astrophysics Data.
19. Eckert, E. R. G. and Drake, R. M. "Analysis of Heat and Mass Transfer," page 55 and 471, McGraw-Hill, 1972.

Downloaded by Chris Torre on December 30, 2021 | http://arc.aiaa.org | DOI: 10.2514/6.2022-0316

20. Schapiro, A. H., "The Dynamics and Thermodynamics of Compressible Fluid Flow," Ronald Press, 1974, MIT, page 42.
21. Ibid., Carroll and Ostlie, page 415.
22. Cf. also Internet Article, http://hyperphysics.phy-astr.gsu.edu/hbase/Kinetic/shegas.html.
23. Zhuravleva, I., Churazov, E., Schekochihin, A. A., Allen, S. W., Vikhlinin, A. and Werner, N., "Suppressed Effective Viscosity in the Bulk Intergalactic Plasma," Nature Astronomy, June 2019.
24. Brady, P. Ditmire, T., Horton, W., Mays, M. L. and Zakharov, Y., "Laboratory Experiments Simulating Solar Wind Driven Magnetospheres," in Physics of Plasma 16, 2009, University of Texas at Austin. Cf. also Ibid., E. R. G. Eckert and R. M. Drake, page 471.
25. Moffatt, H. Keith, 2000, "Reflections on Magnetohydrodynamics". In: *Perspectives in Fluid Dynamics* (ISBN 0-521-53169-1) (Ed. G.K. Batchelor, H.K. Moffatt & M.G. Worster) Cambridge University Press, p 347–391.
26. Volkov, Alexey, "Non-Equilibrium Gas Dynamics," ME 591, Spring 2017, University of Alabama.
27. Marks, Mariano, "Comparing Langmuir Probe Traces of Different Debye Length-to-Probe Radius Ratios", 2011, *McNair Scholars Research Journal*: Vol. 3: Issue 1, Article 4.
28. Chen, F. F, "Introduction to Plasma Physics and Controlled Fusion." 1984, New York, Plenum Press.
29. Thorne, Kip, "Chapter 20: The Particle Kinetics of Plasma", in *Applications of Classical Physics*. September 7, 2017.
30. Ibid., Sharipov, equa. 20. Cf. also "Flow of Gases through Tubes and Orifices" by R. Gordon Livesey in "*Foundations of Vacuum Science and Technology*," edited by James M. Lafferty, 1998 John Wiley & Sons, Inc.
31. Ibid., Sharipov, p. 5, equa. 20. Cf. also Internet Article, http://fisica.ufpr.br/sharipov/
32. Ibid., Scharipov, p. 5, equa. 19.
33. Genestreti, Kevin J. and Goldstein, Jerry, "Temperature of Plasmasphere from Van Allen Probes HOPE", Trinity University, Physics and Astronomy Dept., Journal of Geophysical Research Space Physics, 122(1),310-323. Doi:10. 1002/2016JA023047. Cf. also "Cosmology," Michael Rowan-Robinson, 2004, 4th edition, Oxford University Press.
34. Ogilvie, G. I., "Lecture Notes on Astrophysical Fluid Dynamics," 2016, University of Cambridge, page 10. Cf. also Wilson, L. B., et.al., "The Statistical Properties of Solar Wind Temperature Parameters Near 1 AU," 2018, *American Astronomical Society*, 2018 June.
35. Cercignani, C., "Rarefied Gas Dynamics," section 7.2 The DSMC Method, p. 231, Cambridge University Press, 2000.
36. Ibid., Sutton and Sherman, p. 154, equation 5.98.
37. Spitzer, Lyman, "Physics of Fully Ionized Gasses", p. 137, equation 5-32, 1962, John Wiley and Sons.
38. Jinsah, Ajth Kirshnan, "Magnetohydrodynamic Power Generation", Government Engineering College, Kozhikode, Kerala, India, International Journal of Scientific and Research Publications, Volume 3, Issue 6, June 2013.
39. Ibid., Sutton and Sherman, p. 154, equation 5.98.
40. Ibid., Jinsah, Ajth Kirshnan.
41. Ibid., Jinsah, Ajth Kirshnan.
42. Internet Article, https://en.wilipedia.org/wiki/solenoid
43. Cf. also Bera, Tushar Kanti "A Magnetohydrodynamic (MHD) Power Generating System: A Technical Review," 2020 *IOP Conf. Ser.: Mater. Sci. Eng.* 955 012075.
44. Julian, R. R., et. al., "Ion Funnels for the Masses: Experiments and Simulations with a Simplified Ion Funnel", Aug. 10, 2005, American Society for Mass Spectrometry.
45. Kelly, R. T., et. al., "The Ion Funnel: Theory, Implementations, and Applications", April 23, 2009, Wiley InterScience.
46. Internet Article, https://en.wikipedia.org/wiki/Mu-metal
47. NASA/TP-2021-0021263, "State of the Art Small Spacecraft Technology," October, 2021.
48. Jones, H. W., "The Recent Large Reduction in Space Launch Cost," NASA Ames, July 10, 2018.
49. JPL D-101316, Solar Power Technologies for Future Planetary Science Missions, December, 2017
50. Benson, Scott, W., "Solar Power for Outer Planets Study", NASA Glenn Research Center, Nov. 8, 2007.
51. "Space Transportation Costs: Trends in Price per Pound to Orbit," Futron Corporation, Sept. 6, 2002.
52. Internet Article, https://space.nss.org/the-case-for-solar-power-from-space/
53. Internet Article, https://www.nasa.gov/feature/new-solar-arrays-to-power-nasa-s-international-space-station-research
54. Internet Article, https://en.m.wikipedia.org/wiki/Space_launch_market_competition
55. Internet Article, https://www.sbir.gov/node/386422

Downloaded by Chris Torre on December 30, 2021 | http://arc.aiaa.org | DOI: 10.2514/6.2022-0316

56. Internet Article, https://en.wikipedia.org/wiki/Cygnus_(spacecraft)
57. Internet Article, https://en.wikipedia.org/wiki/XMM-Newton
58. Internet Article, https://en.wikipedia.org/wiki/LADEE
59. Internet Article, https://en.wikipedia.org/wiki/Parker_Solar_Probe
60. Internet Article, https://archive.ph/20120910210207/http://www.spacenews.com/contracts/091112-dutch-space-build-solar-arrays--cygnus.html
61. Internet Article, https://www.nasa.gov/smallsat-institute/sst-soa/power
62. Internet Article, https://spaceflightnow.com/atlas/av020/090610lcross.html
63. Internet Article, https://en.wikipedia.org/wiki/Dawn_(spacecraft)
64. Internet Article, https://spaceflight101.com/spacecraft/o3b/
65. Internet Article, https://en.wikipedia.org/wiki/Mars_Global_Surveyor

"*Patents*

1. Torre, C. N., and Torre, W. V., Sherwood, AR, U.S. Patent for a "System and Method for Converting Space-Based Ionized Plasma into Electrical Power for Spacecraft Using Magnetohydrodynamic Generation," Application No. 16,949,919, 20 November, 2020.

Downloaded by Chris Torre on December 30, 2021 | http://arc.aiaa.org | DOI: 10.2514/6.2022-0316